Journal of Polymer Research (2020) 27: 301
https://doi.org/10.1007/s10965-020-02255-6

ORIGINAL PAPER

Preparation of thermally stable magnetic poly(urethane-imide) /nanocomposite containing β-cyclodextrin cavities as new adsorbent for lead and cadmium

Hasti Eibagi [1] · Khalil Faghihi [1]

Received: 5 March 2020 / Accepted: 17 August 2020 / Published online: 10 September 2020

Abstract
In this work, the thermally stable magnetic poly(urethane-imide) nanocomposite (β-CDPUIm-MNPs (9)) was prepared by reaction of β-cyclohexatriene with diisocyante (5) as a new synthetic cross linker agent and its adsorption behavior for removal of heavy metal ions from water was examined and compared with bare poly(urethane-imide). This poly(urethane-imide) based nanocomposite was employed for the removal of Pb(II) and Cd(II) metals from the waste water for the first time and it has proved to have an excellent efficiency probably due to the presence of nitrogen and oxygen atoms in the imide ring. β-CDPUIm-MNPs (9) displayed highly effective adsorption performance to lead and cadmium and showed maximum adsorptions during 20 min. For optimization of lead and cadmium ions adsorption, the effects of different factors like pH, contact time, and initial amounts of Pb(II) and Cd(II) ions were studied. Results showed that pH has a great influence on the adsorption behavior and also maximum adsorption capacity was obtained at pH 7. Examination of the isotherm and adsorption kinetics showed that equilibrium adsorptions and kinetic are well-modeled by applying Langmuir isotherm model and pseudo-second-order kinetics, respectively. The maximum adsorption capacities of β-CDPUIm-MNPs (9) for Pb(II) and Cd(II) ions based on Langmuir isotherm calculation were 344.830 and 303.030 mg/g, respectively. Regenerated β-CDPUIm-MNPs (9) were used as adsorbent and show high adsorption capacity without any reductions of magnetic intensity and aggregation of adsorbents under five repeating cycles.

Keywords Poly(urethane-imide) · β-Cyclodextrin · Diisocyanate · Nanocomposite · Adsorbent · Heavy metal

Introduction

Water resources on the earth are valuable and limited. Increasing population and industrialization caused a high reduction in drinking water. 90 Percent of diseases in the developing countries are related to contaminated drinking water [1]. One of the important human health challenges is heavy metal contaminations in water [2, 3]. However many articles have been reported to treatment water resources [4].

Heavy metal ions such as lead and cadmium are toxic and carcinogenic even in small amounts. These heavy metals are not biodegradable in living organisms and caused many diseases in human lifes [5]. Therefore, effective methods to remove heavy metals from water resources are essential. Classical methods to remove heavy metals such as reverse osmosis [6], electrochemical treatment [7], membrane filtration [8], chemical oxidation [9], chemical reduction [10], and ion exchange [11] are expensive and energy-consuming. In addition, some of them create new problems including production of other toxic materials [12]. In order to solve problems provided by above techniques, many efforts have been done to evaluate the efficiency of new adsorbents to removal of pollutants [13]. New adsorption techniques, in addition to being inexpensive, can be applied on a large scale and produce high-quality water without sludge production [14]. Recent researches focus on adsorbents like activated carbons, metal-oraganic frameworks, clays, zeolites, silica beads, biomass and polymeric materials to treat water [15, 16]. In the meantime, carbohydrates have good physical and chemical characteristics, low-prices, easy access and presence of various reactive groups in the main chain show fascinated specific consideration [2]. Biopolymers based on biomolecules such as starch, cyclodextrin, chitin, and chitosan are excellent substitutes for adsorbents due to their specific structure [17–19].

✉ Khalil Faghihi
k-faghihi@araku.ac.ir

[1] Department of Chemistry, Faculty of Science, Arak University, Arak 38156-8-8349, Iran

Current studies show cyclodextrins (CDs) are capable of absorbing pollutants more than zeolites [2] and activated carbon [13]. CDs are very important macrocyclic compounds because they are soluble in water [20], commercially available, inexpensive, nontoxic and readily functionalized [21]. CDs are cyclic oligosaccharides constructed from glucopyranose units connected to each other by α-1,4-linkages [22, 23]. The most usable cyclodextrins include 6, 7 and 8 units of glucopyranose, which are called α-, β- and γ- cyclodextrin respectively [24]. The outer surface of these structures is hydrophilic and their central cavity is lipophilic [25]. The presence of available OH groups in cyclodextrin molecules provides active sites which can form a number of connections [26]. Among them β-cyclodextrin has been more used due to its easy availability, cheapness and more reactivity [27, 28]. However, β-cyclodextrin are soluble in water, which limits their application to water purification [21]. Conversion of β-cyclodextrin to water insoluble materials by cross-linking to polymer networks and production of polymer derivatives or their immobilization on solid supports are proper solutions to this problem [29].

Polyurethanes (PUs) are multipurpose polymers. Unfortunately, they have low thermal stability, which limits their applications [30]. There have always been efforts to improve the thermal stability of polyurethanes. One way to improve the thermal stability of PU is the chemical modification of its structure by blending or copolymerizing with more thermally stable polymers. Poly(urethane-imide)s (PUIm)s are unique polymeric structures known for their interesting mechanical and thermal properties and also for their environmental friendly behaviors [31]. Incorporating symmetric aromatic imide rings with strong bonds into polyurethane backbone of PUIms provide good balances between mechanical and thermal properties and flexibility of these materials [30]. On the other hand introducing nanoparticles with high surface area to polymeric matrix associated with sorption sites improve adsorption ability [32, 33]. Among nanoparticles, magnetic nanoparticles are considered for high surface area and easy separation by external magnetic field [34–36]. Between magnetic nanoparticles, iron oxides such as magnetite (Fe_3O_4) with high saturation magnetizations have super paramagnetic behavior and less toxicity [37, 38]. Magnetite is a cubic mineral found in nature and can easily be synthesized [39]. Therefore, it is supposed that preparation of PUIms containing imide rings and β-cyclodextrin cavities not only provides a new adsorbent with good absorbing ability but also provides a thermally stable adsorbent with good mechanical properties.

The purpose of this research is to apply new friendly magnetic PUIm nanocomposites containing β-cyclodextrin cavities as the absorbent. The more important properties of PUIm nanocomposites are high thermal stability and reusability. Oxygen and nitrogen atoms in the imide and urethane linkages and oxygens in the pyranose rings and in glycoside bonds of β-cyclodextrin moiety may have great effects on the removal of heavy metals leading to the increase of adsorption capacity. The results has shown that these nanocomposites have a great capability to remove lead and cadmium ions from water in the optimized conditions.

Experimental section

Trimellitic anhydride, β-cyclodextrin (β-CD), 4-aminobenzoic acid, triethylamine, sodium azide, and ethyl chloroformate were purchased from Sigma-Aldrich chemical company. *N*,*N*-Dimethyl formamide (DMF), benzene, glacial acetic acid and acetone were from Merck chemical company. The adsorbents were synthesized through several steps as reported in [40].

Fourier transform infrared (FTIR) spectra were recorded on a Perkin Elmer FT-IR spectrophotometer in the range of 400–4000 cm^{-1}. The spectra of solids were obtained by using the KBr pellet technique. ^1H and ^{13}C-NMR spectra were recorded on a Brucker Avance 300 MHz spectrometer in DMSO-d_6 with TMS as an internal standard. BET surface areas were measured by nitrogen adsorption and desorption using a BELSORP-mini II (BEL Japan) system at 77 K. The samples were outgassed for 24 h at 100 °C. Crystal structure of nanocomposites were determined by Philips Xpert Xray powder diffraction (XRD), which diffracts meter (Cu-Kα radiation and λ = 0.15406) in the range of Bragg angle 10–80 by using 0.05 as the step length. The thermogravimetric analysis (TGA) and derivative thermogravimetry (DTG) data for β-cyclodextrin–polyurethane grafted to magnetic nanoparticles were obtained on a Mettler TA4000 system under N_2 in the range of 25–800 °C at a heating speed of 10 °C min^{-1} by Tescan mira Π. Morphology and nanoparticles size of resulting nanocomposites were considered by Field emission scanning electron microscope (Mira 3-XMU). The magnetic properties of nanostructures were detected by model 730 vibrating sample magnetometer (VSM) at room temperature.

Synthesis of imide-diacid (3) A mixture of trimellitic anhydride (1) (20 mmol, 3.84 g) and 4-aminobenzoic acid (2) (20 mmol, 2.74 g) in glacial acetic acid (50 mL) were mixed at room temperature overnight and subsequently refluxed at 140 °C for 7 h. Resulting mixture was poured into crushed ice water until white precipitate formed. Then precipitate was filtered off and washed with deionized water to yield pure imide-diacide (3) (5.61 g, 90.19%) [41]. Yield: 90.16%; mp: 275–300 °C, FTIR (KBr, cm^{-1}): 3400–2500 (OH), 1730, 1702, and 1686 (C=O), 1605 and 1512 (C=C), 1485, 1424, 1376, 1299, 1223, 1121, and 1091. ^1H-NMR (DMSO-d_6, 300 MHz): δ 7.62 (d, J = 8.0 Hz, 2H), 8.10 (d, J = 8.1 Hz, 3H), 8.32 (s, 1H), 8.43 (d, J = 7.5 Hz, 1 H) ppm. ^{13}C-NMR

(D_2O, 100 MHz): δ 123.9, 124.4, 127.4, 130.3, 130.6, 132.4, 135.2, 136.0, 137.1166.3, 166.4, 167.2.

Synthesis of diacyl azide (4) Into a 100 mL round-bottomed flask containing of imide-diacide (3) (10 mmole, 3.11 g) in 20 ml of acetone was added drop wise triethylamine (22 mmole, 2.23 g) and stirred about 30 min. Then a solution of ethyl chloroformate (22 mmole, 2.39 g) into 5 ml acetone was added drop wise over 30 min and stirred for another 30 min. Subsequently a solution of sodium azide (25 mmole, 1.62 g) into 15 mL of water was added drop wise to above mixture, and stirred for 2 h. Finally, 100 mL of water was added to the mixture and resulted cream colored diacyl azide (4) was filtered off and dried at ambient temperature. Yield: 80.14%; FTIR (KBr, cm^{-1}): 3104 and 3081 (C-H), 2183 and 2143 (N_3), 1780, 1734, and 1689 (C=O), 1604 and 1511 (C=C), 1418, 1373, 1286, 1260, 1216, 1181, 1121, 1088, 1001.

Synthesis of diisocyanate (5) Into 100 mL round-bottomed flask equipped with a condenser and magnetic stirrer was added diacyl azide (4) (5 mmol, 1.806 g) into 80 mL dry benzene and refluxed for 10 h. The yellow powder of diisocyanate (5) was formed after evaporation of solvent under reduced pressure. Yield: 87.46%; FTIR (KBr, cm^{-1}): 2283 (NCO), 1776 and 1716 (C=O), 1607 and 1537 (C=O), 1461, 1440, 1382, 1280, 1251, 1215, 1126, 1116, 1091.

Synthesis of superparamagnetic nanoparticles (MNPs) (8) In following magnetic nanoparticles (MNPs) were prepared by an improved method such co-precipitation method [42]. Ferrous chloride ($FeCl_2.4H_2O$) (16 mmol, 3.18 g) and ferric chloride ($FeCl_3.6H_2O$) (28 mmol, 7.57 g) were dispersed into 320 mL of deionized water. Initial molar ratios of Fe(II)/Fe(III) is 1/1.75. The mixture was stirred under N_2 atmosphere at 80 °C for 1 h. Then, 40 mL of NH_3 (25%) was quickly added to the mixture, and stirred under N_2 atmosphere for another 1 h and then cooled to room temperature. The precipitated particles were washed five times with hot water and separated by magnetic decantation. Finally, magnetite nanoparticles (8) were dried under vacuum at 70 °C. FTIR (KBr, cm^{-1}): 3411, 1650, 627, 583 (Fe-O).

Synthesis of β-Cyclodextrin poly(urethane-imide) (β-CDPUIm) (7) Into 100 mL round-bottomed flask containing diisocyanate (5) (17.6 mmol, 5.37 g) into dry DMF (15 mL) was gradually added a solution of β-cyclodextrin (6) (1.76 mmol, 2.0 g) into 15 ml of dry DMF and resulting mixture was stirred for 6 h at 70 °C. The final product was washed three times with water and acetone, then filtered and dried under vacuum for 24 h. FTIR (KBr, cm^{-1}): 3350 (N-H and O-H), 1774 and 1710 (C=O), 1606, 1512, 1383. ^{1}H-NMR (DMSO-d_6, 300 MHz): δ 3.64 (bs), 4.37 (bs), 4.51 (bs), 4.90 (bs), 5.42 (bs), 5.10–5.90 (m), 6.99 (s), 7.15–7.95 (m), 9.13 (bs) ppm.

Synthesis of β-cyclodextrin poly(urethane-imide)(7) grafted to Fe_3O_4 magnetic nanoparticles(8) (β-CDPUIm-MNPs)(9) Magnetic nanoparticles (8) (1.73 mmol, 0.40 g) were dispersed into 30 ml dry DMF in a 100 mL round-bottomed flask and then a solution of diisocyanat (5) (17.6 mmol, 5.37 g) into 15 ml of DMF was gradually added into the mixture and stirred for 3 h by a mechanical stirrer. Finally a solution of β-cyclodextrin (6) (1.76 mmol, 2.0 g) into 15 mL of dry DMF was gradually gradually added to the mixture and stirred for 3 h at 70 °C. Resulting β-CDPUIm-MNPs (9) was washed three times with distillated water and acetone, separated by magnetism and dried under vacuum for 24 h [37]. FTIR-(KBr, cm^{-1}): 3366 (N-H and O-H), 3075, 2926, 1774 and 1722 (C=O), 1660, 1606, 1436, 1385 cm^{-1}.

Batch-adsorption studies To optimization of adsorption process of lead and cadmium ions, the effects of different factors like pH, contact time, and initial amounts of Pb(II) and Cd(II) ion were studied. Adsorption experiments were carried out by adding of β-CDPUIm-MNPs (9) (50 mg) to 50 mL conical flasks containing different amounts of Pb(II) and Cd(II) ions. As comparable experiments, similar trials were performed by adding same amounts of β-CDPUIm (7) (50 mg). The flasks were put into a shaking incubator at 180 rpm for different times. Initial pH of samples was adjusted by phosphate

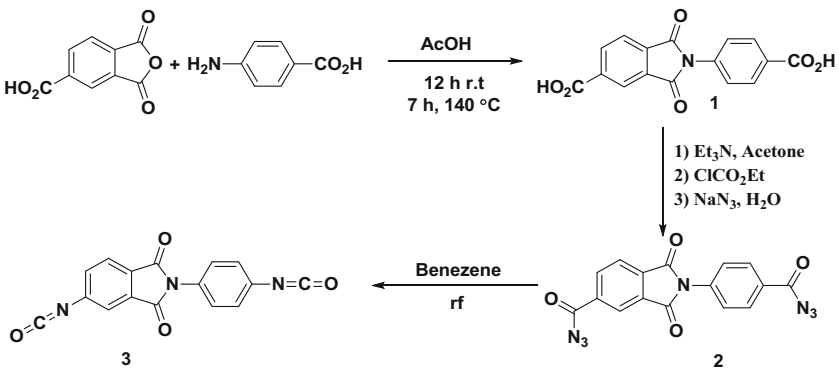

Scheme 1 Synthetic route to preparing diisocyanate (5)

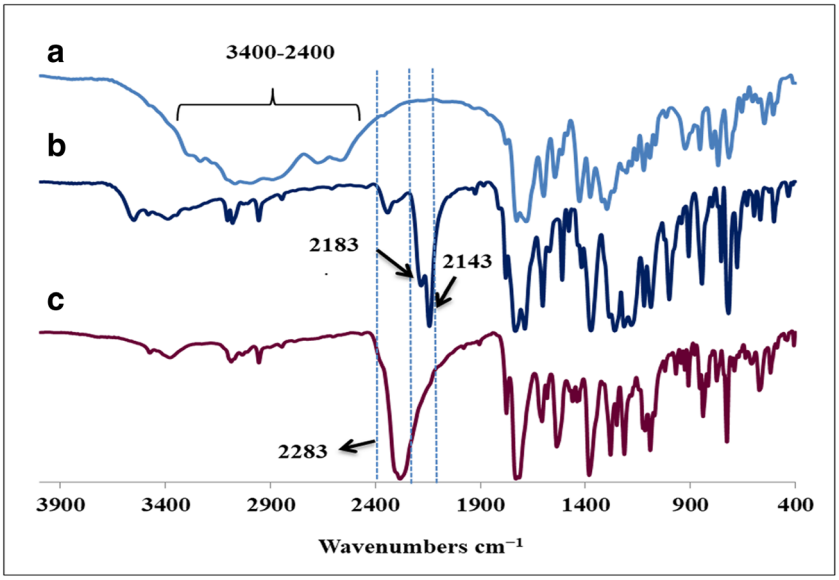

Fig. 1 FT-IR spectra of imid-diacid (3) (**a**), diacyl azide (4) (**b**), and diisocyanate (5) (**c**)

buffers. The Pb(II) and Cd(II) concentrations selected between 100 and 350 mg L^{-1}. Adsorption kinetic analyses evaluated with an initial Pb (II) and Cd(II) concentration about 200 mg L^{-1} at pH 7 with an adsorbent dose of 50 mg. The prepared mixtures were allowed to react with adsorbent for a contact time between 1 and 180 min. At particular time intervals, mixtures were separated by a permanent magnet, filtered and Pb(II) and Cd(II) concentrations were measured. The concentrations of heavy metal ions in the filtrate were measured by atomic adsorption spectroscopy (PerkinElmer AA700, USA). The following Eq. 1 was applied to calculate the adsorption capacity of the adsorbent (q_e, mg/g).

$$q_e = \frac{(C_0 - C_e)V}{m} \quad (1)$$

The investigation of recyclability and reusability of adsorbent

The separation of β-CDPUIm-MNP (9) containing adsorbed Pb(II) and Cd(II) was carried out by a permanent magnet and then it was washed with water. Then, in order to regenerate β-CDPUIm-MNPs (9), desorption phenomenon was carried out by treating used adsorbents with nitric acid solution under stirring. Finally, the recovered β-CDPUIm-MNPs (9) was ready to be reused for other adsorption-desorption tests after being dried.

Results and discussion

Synthesis and characteristics of β-CDPUIm (7) and β-CDPUIm-MNPs (9)

Polyurethane (PU) skeletons are usually prepared by polycondensational reaction of a diol or polyol reagent with diisocyanate or poly isocyanate compounds. Different methods have been reported to prepare isocyanates, including phosgenation of an amine or its salts [43], oxidation of isonitriles [44], and conversion of hydroxamate via the Lossen rearrangement [45]. Oxidative rearrangements of acyl azides to corresponding isocyanate via the Curtius

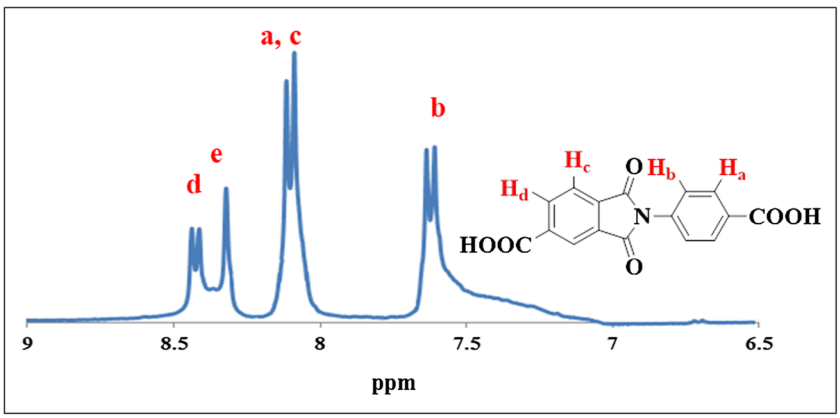

Fig. 2 ^{1}H-NMR spectra of the imid-diacid (3)

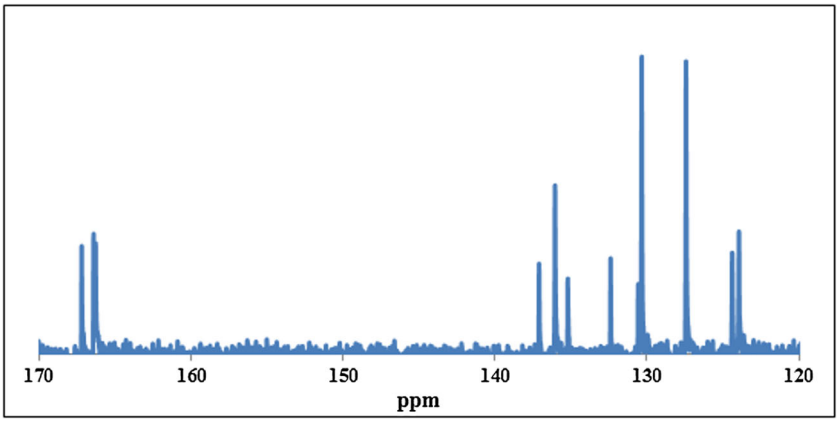

Fig. 3 ^{13}C NMR spectra of the imid-diacid (3)

rearrangements have been used extensively to prepare various isocyanates. Hence, preparations of poly(urethane-imide)s (PUIm)s need proper diols and diisocyanate compound. Our initial investigation began with preparation of a new diisocyanate (5) containing dimide rings as a proper monomer to prepare new poly(urethane-imide) (7) containing β-cyclodextrine cavities. First imide-diacid (3) was obtained by condensational reaction of trimellitic anhydride (1) and 4-aminobenzoic acid (2) in glacial acetic acid according to a typical procedure [41]. Then imide-diacid (3) was converted to diacyl azide (4) by reaction with ethylchloroformate, sodium azide in the presence of triethylamine. Curtius rearrangement of diacyl azide (4) by refluxing in dry benzene yielded diisocyanate (5) (Scheme 1).

The FT-IR spectra of imide-diacid (3), diacyl azide (4), and diisocyanate (5) are shown in Fig. 1. In the FT-IR spectrum of imid-diacid (3) vibrational bands between 3400 and 2400 cm^{-1} are dominated by broad hydrogen bonding bands. The frequencies appeared at 1770, 1722, and 1680 cm^{-1} are corresponding to asymmetric and symmetric vibrations of carbonyl imide rings and also carboxylic moiety, respectively. In FT-IR spectrum of diacyl azide (4), absorption bands at 2183 and 2143 cm^{-1} are related to azide stretching vibrations and also corresponding OH stretching frequencies of carboxylic groups are dispread. Appearance of broad strong isocyanate bands at 2283 cm^{-1} and disappearance of bands related to azide groups clearly confirmed formation of diisocyanate (5).

Also successful fabrication of imid-diacid (3) was confirmed by ^1H-NMR spectroscopy. ^1H NMR spectrum of imid-diacid (3) in DMSO-d_6 exhibited two doublet peaks at 7.62 and 8.43 ppm related to H_b and H_d protons respectively. The singlet peak at 8.32 ppm was attributed to H_e proton of imide ring. Finally, H_a and H_c appeared as one doublet peak at 8.10 ppm due to similarity in their chemical shift (Fig. 2).

The ^1H-decoupled ^{13}C NMR spectrum of imid-diacid (3) shows three carbonyl groups at 166.3, 166.4, and 167.2 ppm. Also appearance of 10 distinct signals in the aromatic region of ^{13}C NMR spectrum of imid-diacid (3) is in good agreement with the proposed structure (Fig. 3).

Also β-Cyclodextrin poly(urethane-imide) (β-CDPUIm) (7) was synthesized by reaction of β-CD (6) with diisocyanate (5) as a cross-linking agent. The urethane linkages were made by nucleophilic addition of two hydroxyl groups of β-CD (6) species onto isocyanate moieties (Scheme 2). The chemical structure of the soluble β-CDPUIm (7) was confirmed by FT-IR and ^1H-NMR analyses.

Taking the benefits of magnetic targeting, Fe_3O_4 nanoparticles (8) were prepared by improved coprecipitation method of an aqueous mixture of Fe(II) and Fe(III) chloride in the presence of ammonia solution. Resulting β-CDPUIm-MNPs (9) were obtained by a two steps-reaction. First isocyanate functionalized MNPs (8) were formed by reaction of free hydroxyl groups onto the surface of magnetic Fe_3O_4 nanoparticles with an excess of diisocyanate (5) and then, insoluble and cross-linked β-CDPUIm-MNPs (9) containing β-CD cavities were prepared by reaction of β-CD (6) with free isocyanate moiety onto MNPs (8) surfaces and also unreacted diisocyanate (5) into dry DMF at 70 °C under nitrogen atmosphere (Scheme 3).

The FT-IR spectra of β-CD (6), β-CDPUIm (7), β-CDPUIm-MNPs (9) and Fe_3O_4 nanoparticles (8) were shown in Fig. 4. FT-IR spectrum of β-CD (6) show a broad

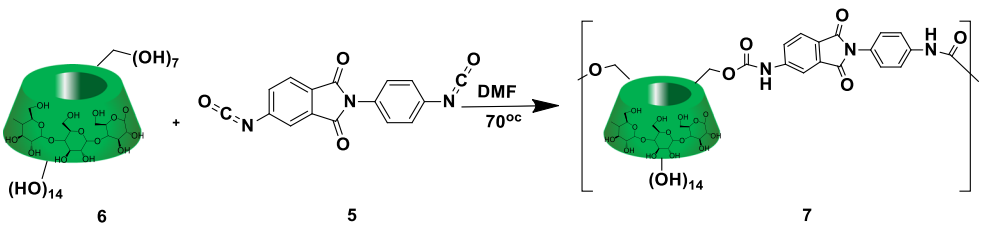

Scheme 2 Synthesis of β-CDPUIm (7)

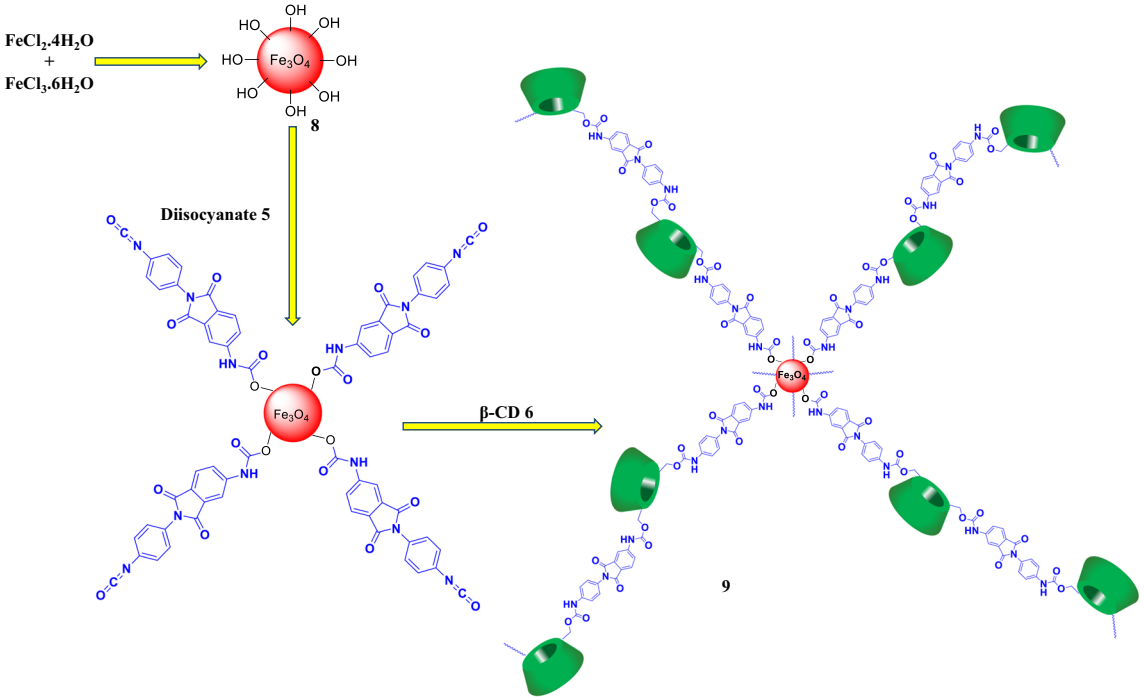

Scheme 3 Synthetic route of β-CDPUIm-MNPs (9) grafted onto Fe_3O_4 magnetic nanoparticles (8)

absorption peak around 3000–3600 cm^{-1} which related to hydroxyl groups of β-CD molecules. Peak appeared around 583 cm^{-1} in pristine Fe_3O_4 (8) spectrum as characteristic absorption of Fe-O was shifted to 593 cm^{-1} after surface modification by β-CDPUIm (7). Disappearance of a strong peak around 2283 cm^{-1} related to diisocyanate (5) moiety in FT-IR spectra of β-CDPUIm (7) and β-CDPUIm-MNPs (9) confirmed completed polymerization. The FT-IR spectrum of β-CDPUIm-MNPs (9) showed characteristic absorption bands at 3366 and 1774, 1722, 1660 cm^{-1} corresponded to NH and C=O starching vibrations. The NHCO stretching frequency was also observed at 1543 cm^{-1}.

The ^{1}H-NMR spectra of β-CD (6) and soluble β-CDPUIm (7) compared in Fig. 5. Appeared protons in high-field (3.11–5.57 ppm) are related to β-CD (6) ring and also appeared signals around 7.15–7.95 ppm are related to aromatic protons. Also two peaks at 6.99 and 9.13 ppm related to N-H of amide moiety confirm formation of urethane linkages in soluble β-CDPUIm (7).

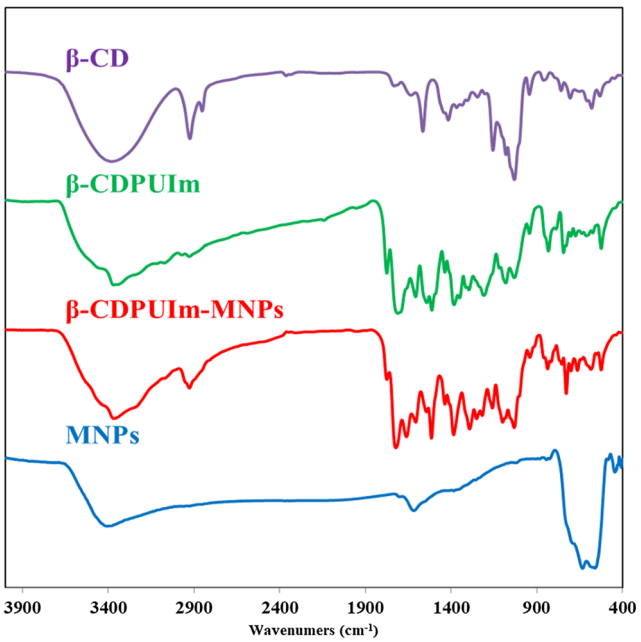

Fig. 4 IR spectra of β-cyclodextrin (6), β-CDPUIm (7), β-CDPUIm-MNPs (9), and Fe_3O_4 nanoparticles (8)

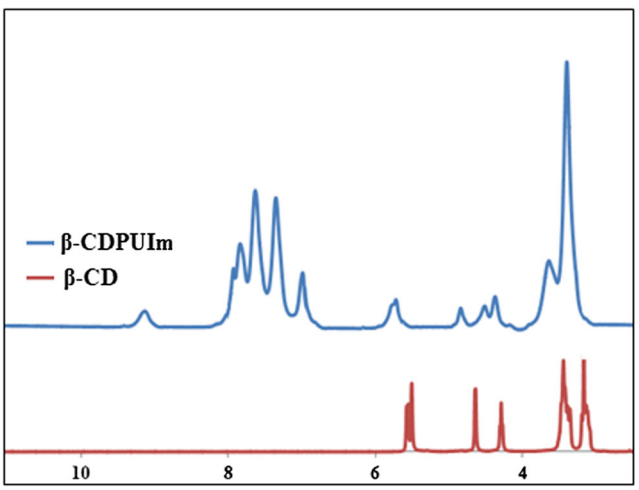

Fig. 5 ^{1}HNMR spectra of β-CD (6) and β-CDPUIm (7)

Brunauer–Emmett–teller (BET) analysis

The specific surface areas of the β-CDPUIm (7) and the β-CDPUIm-MNPs (9) were determined by the Brunauer–Emmett–Teller (BET) surface area analyzer. The results are given in Table 1. The surface area of the β-CDPUIm (7) increased from 0.8336 to 1.9705 m^2/g with the addition of Fe_3O_4 nanoparticles.

XRD analysis

Crystalline structures of Fe_3O_4 nanoparticles (8), β-cyclodextrin poly(urethane-imide) (β-CDPUIm) (7) and β-cyclodextrin poly(urethane-imide) bonded to Fe_3O_4 nanoparticles (β-CDPUIm-MNPs) (9) were clearly visible in XRD measurements in Fig. 6. Six characteristic diffraction peaks of pure Fe_3O_4 (8) are exhibited at $2\theta = 30.2°$, 35.5°, 43.3°, 53.6°, 57.0° and 62.6° which corresponded to (220), (311), (400), (422), (511), and (440) planes of Fe_3O_4 (8), respectively [46]. Comparing XRD pattern of β-CDPUIm (7) to reported XRD pattern of pure β-CD [47] exhibited when the β-CD (6) is combined in a polymer backbone it totally loses its crystalline nature and spread in the poly(urethane-imide) matrix without creating any aggregates. The XRD pattern of β-CDPUIm-MNPs (9) demonstrated corresponding peaks of Fe_3O_4 (8) along with the peaks of β-CDPUIm (7).

TGA and DTG analysis

TGA and DTG analysis of final adsorbent (9) shown in Fig. 7, was used to estimate thermal stability of β-CDPUIm-MNPs (9). There is a five-stage degradation pattern in the range of 30–700 °C in TGA thermogram. First weight loss around 2.89% up to 170 °C suggests a removal process of physically adsorbed water and dehydration of hydroxyl functional groups onto magnetic nanoparticles surfaces. The second weight loss step about 22.50% in the region of 170–390 °C corresponded to the cleavage of the urethane linkages. Another stage of degradation in the region of 390–480 °C is probably related to bond cleavage between β-CD (6), poly(urethane-imde) and magnetic nanoparticles (8). The degradation in the region of 480–600 °C may be related to decomposition of CD. Finally, weight loss in the range of 600–750 °C is related to degradation of magnetic nanoparticles of Fe_3O_4 (8).

Table 1 Comparison of the BET surface area of β-CDPUIm (7) and the β-CDPUIm-MNPs (9)

Samples	Surface Area m^2/g
β-CDPUIm (7)	0.8336
β-CDPUIm-MNPs (9)	1.9705

Field emission scanning electron microscopy (FE-SEM) analysis

By using Field Emission Scanning Electron Microscopy (FE-SEM), morphology and distribution quality of β-CDPUIm (7) and β-CDPUIm-MNPs (9) are identified. Nanoparticles appeared in resulting samples as shown in Fig. 8 show spherical shapes means a large surface area. Size of magnetic nanoparticles is about 200 nm and nanoparticles were homogeneously distributed in resulting samples.

Vibrating sample magnetometer (VSM) analysis

Magnetic property of pure magnetic nanoparticles (Fe_3O_4) (8) and β-cyclodextrin poly(urethane-imide) bonded to magnetic nanoparticles (β-CDPUIm-MNPs) (7) studied with vibrating sample magnetometer (VSM) at room temperature (Fig. 9). The hysteresis loops obtained at room temperature under applied magnetic field were between −10,000 to 10,000 Oe. Resulting saturation magnetization (Ms) value of β-CDPUIm-MNPs (9) was near to 33.0 emu/g at room temperature, and show a suitable view related to frequent magnetic separation. Indeed, this data was less than Ms. of pure Fe_3O_4 (46 emu/g). Remanence magnetization (Mr) values of nano pristine Fe_3O_4 (8) and β-CDPUIm-MNPs (9) were about 9 and 3, respectively and also their coercivity (Hc) were about 0.75 and 0.25, respectively indicating resulting β-CDPUIm-MNPs (9) retained super paramagnetic behavior. Also measuring saturation magnetization (MS) data show super paramagnetic behavior means nano pristine Fe_3O_4 (8) is not damaged during the preparation of β-CDPUIm-MNPs (9). Attaching Fe_3O_4 (8) onto β-cyclodextrin poly(urethane-imide) (7) surfaces leads easy separation of resulting product (β-CDPUIm-MNPs) (9) from water environment by a simple magnetic and reused to successive purification cycles.

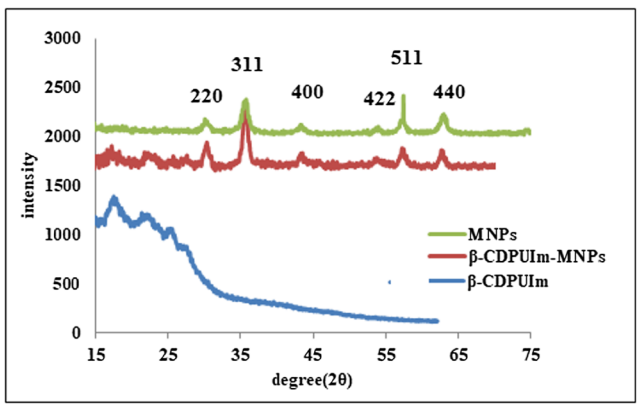

Fig. 6 XRD patterns of bare Fe_3O_4 nanoparticles, β-CDPUIm-MNP (9), and β-CDPUIm (7)

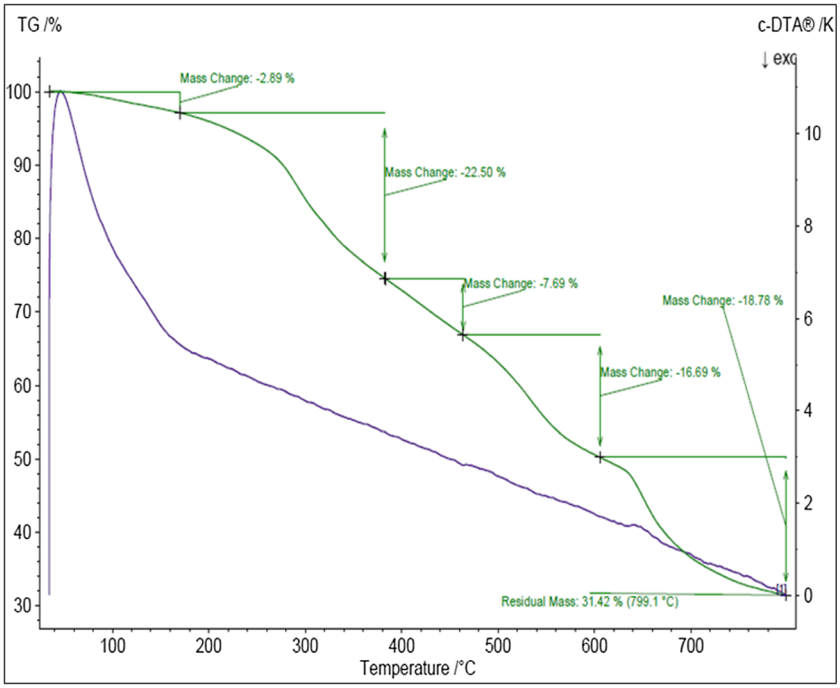

Fig. 7 TGA and DTG analysis of β-CDPUIm-MNPs (9)

Synthetic β-CDPU-MNPs (9) has moderately higher Ms. value in comparison to most reported composite polymers [37]. The high saturation magnetization (Ms) value modifies water purification technique.

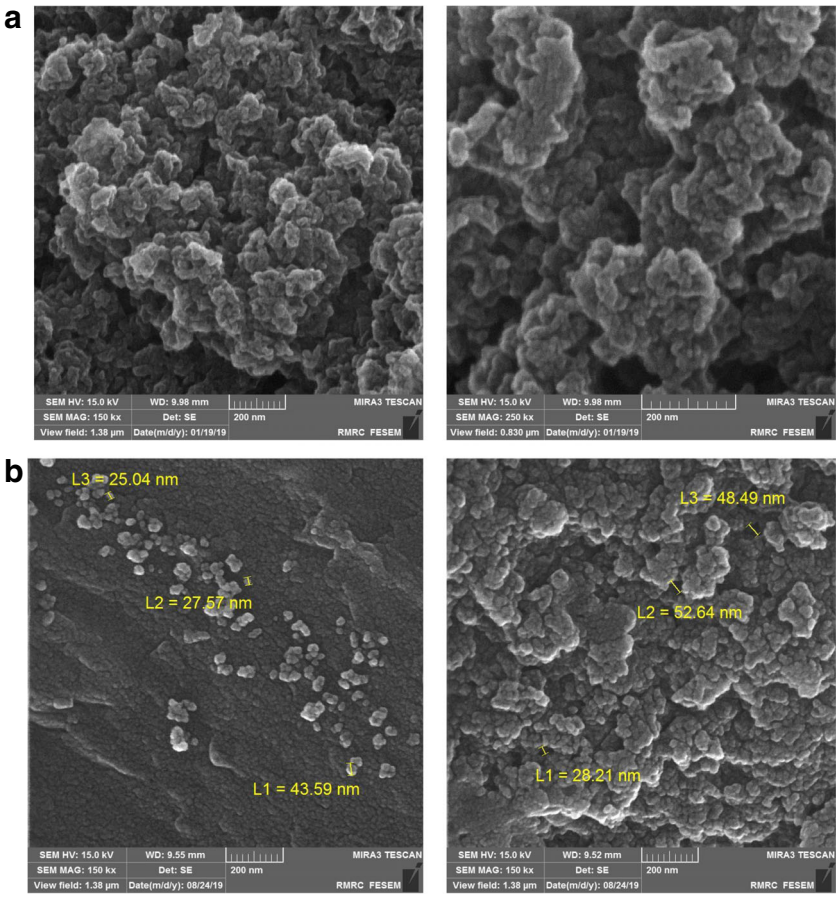

Fig. 8 SEM morphology of β-CDPUIm (7) (**a**) and β-CDPUIm-MNP (9) (**b**)

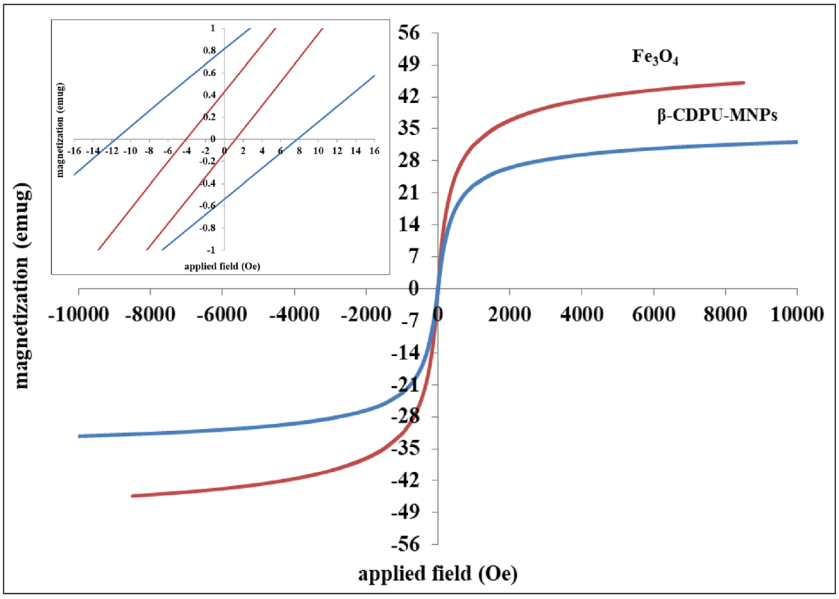

Fig. 9 VSM data of pristine Fe_3O_4 nanoparticles (8) and β-CDPUIm-MNPs (9)

Effect of pH

Adsorption performance depends on pH value of solution because changing of pH leads to different protonation of active sites onto adsorbent surfaces and also effect on adsorption behavior of resulting β-CDPUIm-MNPs (9) to removal of Cd(II) and Pb(II) spices. All of experiment takes placed between pH 2 to 7 at room temperature and resulting data shown in Fig. 10. Results show the removal contents of Cd(II) and Pb(II) spices by β-CDPUIm-MNPs (9) adsorbent were strongly dependent to pH value. Adsorption efficiency of above ions was increased by changing pH value from 2 to 7. The effects of pH on the adsorption of heavy metal ions on β-CDPUIm-MNPs (9) adsorbents can be attributed to electrostatic interaction. In acidic pH active sites become protonated and the absorption of heavy metals decreases.

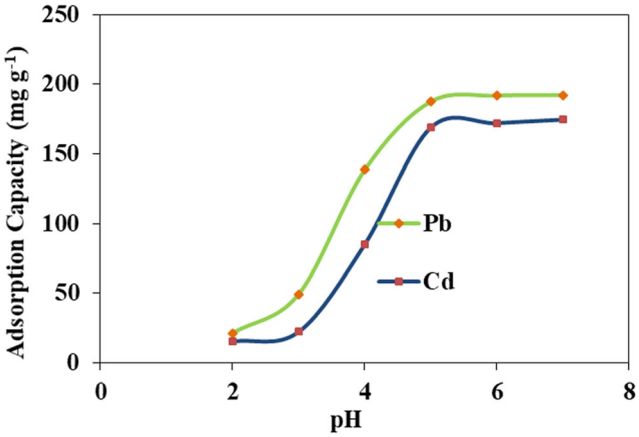

Fig. 10 pH effect on adsorption behavior of Cd(II) and Pb(II) spices

Adsorption isotherms

The absorbance process of heavy metal ions by resulting solid adsorbents is usually verified through the Langmuir and Freundlich isotherms due to their simplest operation. The Langmuir isotherm presumes that maximum adsorption happens when a saturated monolayer of adsorbed molecules is present onto adsorbent surfaces [48]. In contrast to Langmuir isotherm, Freundlich isotherm model is used to depict multilayer adsorption. So, we used these models to lead and cadmium ions uptake onto β-CDPUIm-MNPs (9) and the linear Eq. 2 for Langmuir isotherm model is shown as follows:

$$\frac{C_e}{q_e} = \frac{1}{K_L q_m} + \frac{C_e}{q_m} \quad (2)$$

The Freundlich isotherm model is based on this assumption that adsorption energy depends to contents of occupied adjacent sites and mathematical formula can be expressed in Eq. 3.

$$\ln q_e = \frac{1}{n}\ln C_e + \ln K_F \quad (3)$$

C_e (mg/L) is concentration of heavy metals at equilibrium; q_e (mg/g) is quantity of adsorbed quantity per mass of β-

Table 2 Adsorption isotherm parameters of Pb(II) and Cd(II) onto β-CDPUIm-MNPs (9)

	Langmiure model			Freundlich model		
Metal ion	q_{max} (mg/g)	K_L (L/mg)	R^2	K_F	N	R^2
Pb(II)	344.830	0.160	0.9999	79.040	2.610	0.9416
Cd(II)	303.030	0.058	0.9993	10.380	2.490	0.9661

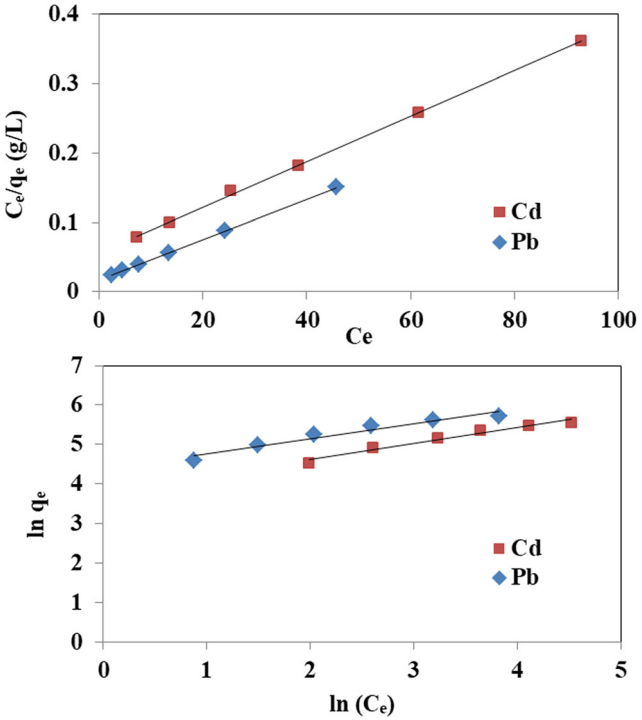

Fig. 11 Langmuir and Freundlich isotherm of adsorption of Pb(II) and Cd(II) onto β-CDPUIm-MNPs (9)

CDPU-MNPs (9); q_m (mg/g) is maximum adsorption capacity at equilibrium, K_L (L/mg) is Langmuir adsorption constant. K_F and n are defined as Freundlich constants related to adsorption capacity and adsorption intensity, respectively.

By plotting the diagram of $\ln q_e$ vs $\ln C_e$, estimations of n and K_F can be accessed by slope and intercept, respectively. Also, the graph of C_e/q_e vs C_e leads to a straight line with slope of $1/q_m$ and intercept of $1/K_L q_m$.

Resulting parameters of Langmuir and Freundlich isotherms calculated by means of linear fitting listed in Table 2 and show in Fig. 11.

Table 3 Comparison of the maximum adsorption capacity of Pb(II), and Cd(II) ions on various adsorbents

Adsorbent	Metal ions	q_{max} (mg/g)	Refs
Magnetic graphene oxide	Cd(II)	91.29	[49]
DTPA/MGO	Cd(II)	286.56	[50]
kapok-DTPA	Cd(II)	163.7	[51]
β-cyclodextrin polymer	Cd(II)	136.43	[52]
β-CDPUIm-MNPs (**9**)	Cd(II)	303.030	This study
Fe_3O_4@SiO_2@mC-H_2O_2	Pb(II)	156	[53]
PU	Pb(II)	236.5	[54]
Magnetic chitosan/graphene oxide	Pb(II)	76.41	[55]
β-cyclodextrin polymer	Pb(II)	196.42	[52]
β-CDPUIm-MNPs (**9**)	Pb(II)	344.830	This study

The maximum adsorption capacity (q_m) values calculated from the Langmuir model were 344.830 and 303.030 mg/g for Pb(II) and Cd(II) ions, respectively. Comparing q_m values of Pb(II) and Cd(II) ions adsorption to other reported adsorbents (Table 3) showed that the β-CDPUIm-MNPs (9) have a higher adsorption capacity.

The adsorption of Cd(II) and Pb(II) on adsorbent might be related to complexation and electrostatic interactions between Cd(II) and Pb(II) and oxygen and nitrogen- containing groups on β-CDPUIm backbone [56]. This is in accordance with Langmuir model. Poly(urethane-imide) backbone will be ionized at acidic pH. Therefore, protonation of the amine and carbonyl groups causes the electrostatic repulsion between the positive charges on the poly(urethane-imide) and Cd(II) and Pb(II), which lead to the less adsorption of them. In neutral medium the free carbonyl and nitrogen groups interacted with Cd(II) and Pb(II) and hence adsorption capacities will be increased. Hence, acid treatment is a proper method for regeneration of adsorbent.

Adsorption kinetics

The adsorption contents of Pb(II) and Cd(II) by β-CDPUIm (7) and β-CDPUIm-MNPs (9) adsorbents in aqueous solution versus contact times are shown in Fig. 12.

Results show adsorption capacity of both metal ions by adsorbent increased by increasing the contact time. Also rate

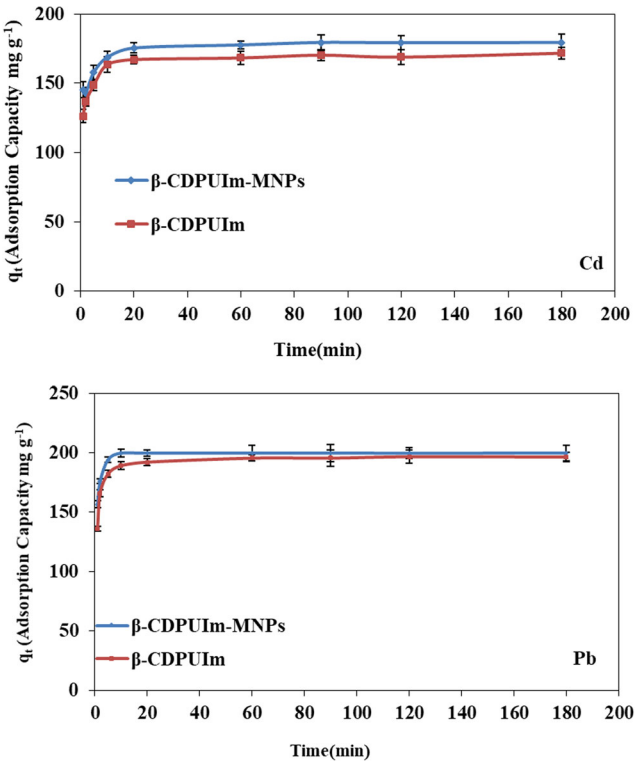

Fig. 12 Effect of adsorption time on the adsorption amount of Pb(II) and Cd(II) by β-CDPUIm-MNPs (9) adsorbent

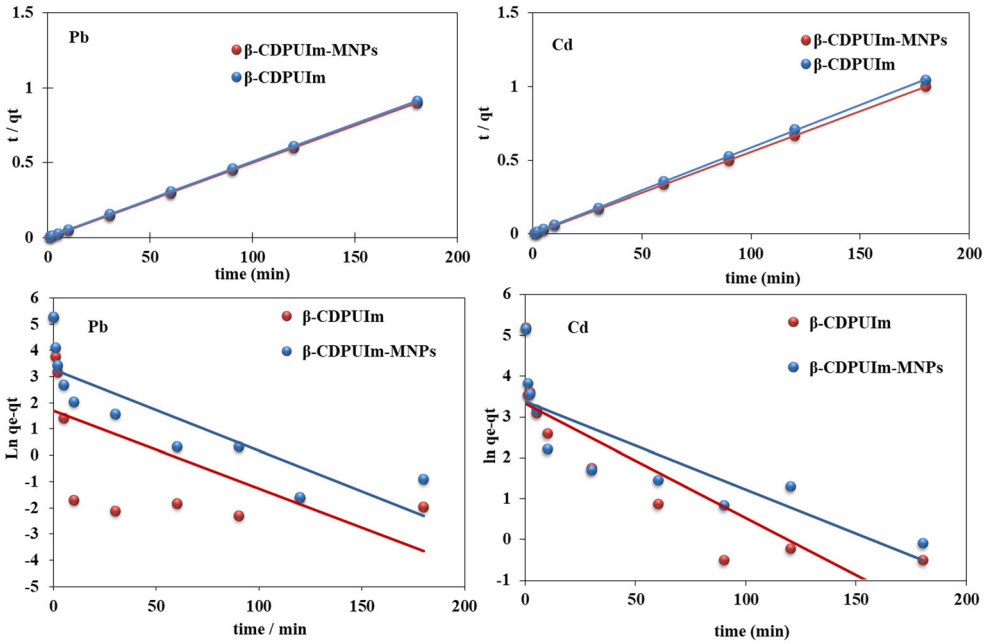

Fig. 13 Pseudo-first-order and pseudo-second-order kinetics of Pb(II) and Cd(II) adsorption by β-CDPUIm (7) and β-CDPUIm-MNPs (9)

of adsorption was remarkable fast and maximum adsorption attained within 20 min which is dramatically short time in compare to previous works. β-CDPUIm-MNPs (9) could adsorb heavy metal ions by aqueous solution due to high specific surface area and ability of internal diffusion.

Herein, pseudo-first-order and pseudo-second-order models were examined to find real kinetic model. The pseudo-first-order Eq. 4 is described as follow:

$$\ln(q_e - q_t) = lnq_e - k_1 t \tag{4}$$

The Pseudo-second-order model Eq. 5 is expressed as follow:

$$\frac{t}{q_t} = \frac{1}{k_2 q_e^2} + \frac{1}{q_e} t \tag{5}$$

q_e (mg/g) and q_t (mg/g) are adsorption capacity at equilibrium situation and time reaction respectively; K_1(1/min) and K_2 (mg/g min) are the constant rates of pseudo-first-order and pseudo-second-order models respectively [57, 58].

K_1 and q_e are determined by slope and intercept of linear plot of ln (q_e-q_t) versus time. By plotting the diagram of time/q_t versus time, k_2 and $q_{e,cal}$ can be approximated by intercept and slope respectively (Fig. 13).

Corresponding adsorption kinetics parameters by these models are shown in Table 4.

The adsorption behavior of both samples, fits well to pseudo-second-order model with a high value of correlation coefficient (R^2) (>99%), and also q_e values calculated by pseudo-second-order model are much closer to experimental resulting q_e compare to estimated data by pseudo-first-order model.

Desorption studies

Recycling and reuse of adsorbent are essential to practical and industrial applications. In this research β-CDPUIm-MNP (9)

Table 4 Adsorption kinetic parameters of Pb(II) and Cd(II) onto magnetic adsorbent

Adsorbent	Metal ion	Pseudo-first-order			pseudo-second-order			
		$q_{e,cal}$ (mg/g)	K_1 (1/min)	R^2	$q_{e,cal}$ (mg/g)	K_2 (g/mg min)	R^2	$q_{e,exp}$ (mg/g)
β-CDPUIm-MNPs(**9**)	Pb(II)	26.360	0.031	0.7529	200.000	0.0500	0.9999	192.300
β-CDPUIm(**7**)	Pb(II)	5.450	0.030	0.4017	196.080	0.0217	0.9999	186.530
β-CDPUIm-MNPs(**9**)	Cd(II)	29.560	0.022	0.7111	178.5700	0.0098	0.9998	174.620
β-CDPUIm(**7**)	Cd(II)	28.110	0.028	0.7686	172.41	0.0086	0.9999	165.490

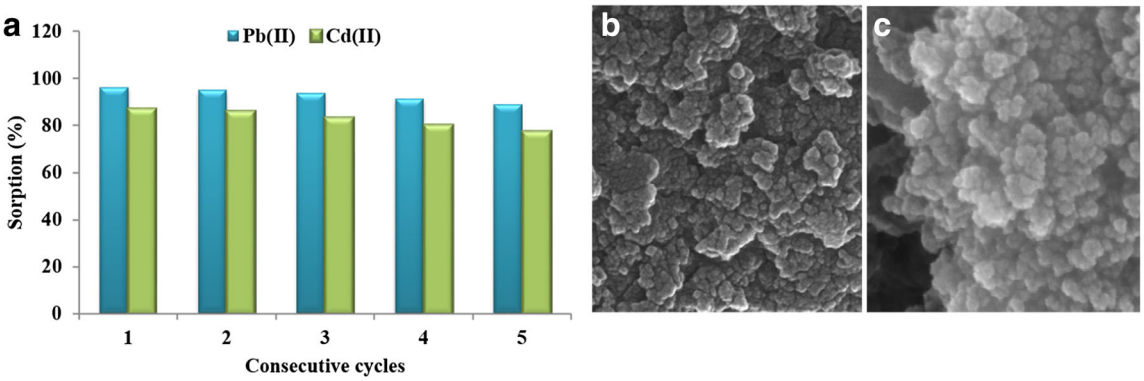

Fig. 14 Performance of β-CDPUIm-MNPs (9) for five cycles of regeneration (**a**) and SEM images of fresh (**b**) and regenerated (**c**) β-CDPUIm-MNP (9) adsorbent

containing adsorbed Pb(II) and Cd(II) were separated by a permanent magnet and washing by water. Results show that prepared β-CDPUIm-MNPs (9) have a weak adsorption capacity at acidic pH means acid treatment is probably a proper method for regeneration of β-CDPUIm-MNPs (9). Therefore, desorption phenomenon takes place by treating isolated adsorbents with nitric acid solution under stirring. Recovered β-CDPUIm-MNPs (9) was dried and applied to other adsorption-desorption tests and desorption efficiency was found about 95%. The adsorption capacity of β-CDPUIm-MNPs (9) against Pb(II) and Cd(II) after five cycling usages decreased about 7.6% and 11.1%, respectively which is probably related to some inactive sites created onto nanocomposites surfaces during the adsorption-desorption processes.

Figure 14 shows representative SEM images of fresh and regenerated β-CDPUIm-MNPs (9) after five cycling usages. The regenerated adsorbents still showed similarity to fresh structure. Resulting magnetic nanocomposite can be simply recycled and reused within several times, which supports their long-time application in water treatment.

Conclusions

In this research, a new magnetic and thermally stable poly(-urethane-imide) as adsorbent containing β-cyclodextrin cavities was successfully prepared and used to remove heavy metals such as lead and cadmium from contaminated water. The adsorption capacity of this adsorbent was significantly enhanced by binding to iron nanoparticles and also easily separated by external magnetic field. The highest amounts of lead and cadmium removal occurred within 20 min and also highest adsorption capacity occurred at pH 7. The equilibrium isotherm data show adsorbent follows the Langmuir model and kinetics of lead and cadmium adsorption pursues the pseudo-second-order model. The maximum adsorption capacities of β-CDPUIm-MNPs for Pb(II) and Cd(II) ions based on Langmuir isotherm calculation were 344.830 and 303.030 mg/g, respectively. In addition, β-CDPUIm-MNPs (**9**) can be recycled up to five times without any significant reduction in its magnetic intensity and adsorption capacity. The adsorption capacity of β-CDPUIm-MNPs (**9**) against Pb(II) and Cd(II) after five cycling usages decreased about 7.6% and 11.1%, respectively. Based on these resulting data magnetic β-CDPUIm-MNPs (**9**) can be a potentially proposed as suitable adsorbent to removal of heavy metal ions from aqueous media.

Acknowledgments We appreciate financial support of Research Concil of Arak University.

References

1. Bora T, Dutta J (2014) Applications of nanotechnology in wastewater treatment—a review. J Nanosci Nanotechnol 14(1):613–626
2. Badruddoza AZM, Shawon ZBZ, Tay WJD, Hidajat K, Uddin MS (2013) Fe3O4/cyclodextrin polymer nanocomposites for selective heavy metals removal from industrial wastewater. Carbohydr Polym 91(1):322–332
3. Li T, Liu X, Li L, Wang Y, Ma P, Chen M, Dong W (2019) Polydopamine-functionalized graphene oxide compounded with polyvinyl alcohol/chitosan hydrogels on the recyclable adsorption of cu (II), Pb (II) and cd (II) from aqueous solution. J Polym Res 26(12):281
4. Abdolmaleki A, Mallakpour S, Mahmoudian M, Sabzalian MR (2017) A new polyamide adjusted triazinyl-β-cyclodextrin side group embedded magnetic nanoparticles for bacterial capture. Chem Eng J 309:321–329. https://doi.org/10.1016/j.cej.2016.10.063
5. Ozay O, Ekici S, Baran Y, Aktas N, Sahiner N (2009) Removal of toxic metal ions with magnetic hydrogels. Water Res 43(17):4403–4411
6. Imiete IE, Viacheslovovna Alekseeva N (2018) Reverse osmosis purification: a case study of the Niger Delta region. Water Sci 32(1):129–137
7. Hunsom M, Pruksathorn K, Damronglerd S, Vergnes H, Duverneuil P (2005) Electrochemical treatment of heavy metals (Cu2+, Cr6+, Ni2+) from industrial effluent and modeling of copper reduction. Water Res 39(4):610–616
8. Ansari A, Vahedi S, Tavakoli O, Khoobi M, Faramarzi MA (2019) Novel Fe3O4/hydroxyapatite/β-cyclodextrin nanocomposite

adsorbent: synthesis and application in heavy metal removal from aqueous solution. Appl Organomet Chem 33(1):e4634
9. Seo S, Sung B, Kim G, Chu K, Um C, Yun S, Ra Y, Ko K (2010) Removal of heavy metals in an abandoned mine drainage via ozone oxidation: a pilot-scale operation. Water Sci Technol 62(9):2115–2120
10. Walker DJ, Hurl S (2002) The reduction of heavy metals in a stormwater wetland. Ecol Eng 18(4):407–414
11. Dąbrowski A, Hubicki Z, Podkościelny P, Robens E (2004) Selective removal of the heavy metal ions from waters and industrial wastewaters by ion-exchange method. Chemosphere 56(2):91–106
12. Rima J, Assaker K (2013) B-Cyclodextrin polyurethanes copolymerised with beetroot fibers (bio-polymer), for the removal of organic and inorganic contaminants from water. J Food Res 2(1):150
13. Taka AL, Pillay K, Mbianda XY (2017) Nanosponge cyclodextrin polyurethanes and their modification with nanomaterials for the removal of pollutants from waste water: a review. Carbohydr Polym 159:94–107
14. Gupta VK, Ali I, Saini VK (2007) Defluoridation of wastewaters using waste carbon slurry. Water Res 41(15):3307–3316
15. Crini G (2005) Recent developments in polysaccharide-based materials used as adsorbents in wastewater treatment. Prog Polym Sci 30(1):38–70
16. Shayegan H, Ali GAM, Safarifard V (2020) Recent Progress in the removal of heavy metal ions from water using metal-organic frameworks. ChemistrySelect 5(1):124–146. https://doi.org/10.1002/slct.201904107
17. Zhuang S, Yin Y, Wang J (2018) Simultaneous detection and removal of cobalt ions from aqueous solution by modified chitosan beads. Int J Environ Sci Technol 15(2):385–394
18. Wang J, Zhuang S (2017) Removal of various pollutants from water and wastewater by modified chitosan adsorbents. Crit Rev Environ Sci Technol 47(23):2331–2386
19. Wang J, Chen C (2009) Biosorbents for heavy metals removal and their future. Biotechnol Adv 27(2):195–226
20. Cathum SJ, Boudreau A, Obenauf A, Dumouchel A, Brown CE, Punt M (2006) Treatment of mixed contamination in water using cyclodextrin-based materials. Remediat J 16(4):43–56
21. Mirzajani R, Pourreza N, Najjar SSA (2014) β-Cyclodextrin-based polyurethane (β-CDPU) polymers as solid media for adsorption and determination of Pb (II) ions in dust and water samples. Res Chem Intermed 40(8):2667–2679
22. Tudisco C, Oliveri V, Cantarella M, Vecchio G, Condorelli GG (2012) Cyclodextrin anchoring on magnetic Fe3O4 nanoparticles modified with phosphonic linkers. Eur J Inorg Chem 2012(32):5323–5331
23. Xie A, Zhang M, S-i I (2016) Influence of β-cyclodextrin on morphologies and chemical, thermal, and mechanical properties of non-chain extended polyurethane elastomers. J Polym Res 23:1–9
24. Ogoshi T, Harada A (2008) Chemical sensors based on cyclodextrin derivatives. Sensors 8(8):4961–4982
25. Dardeer HM (2014) Importance of cyclodextrins into inclusion complexes. Int J Adv Res 2(4):414–428
26. Morin-Crini N, Crini G (2013) Environmental applications of water-insoluble β-cyclodextrin–epichlorohydrin polymers. Prog Polym Sci 38(2):344–368
27. Mhlanga SD, Mamba BB, Krause RW, Malefetse TJ (2007) Removal of organic contaminants from water using nanosponge cyclodextrin polyurethanes. J Chem Technol Biotechnol 82(4):382–388
28. Kumar A, Kumari A, Asu S, Laha D, Kumar Sahu S (2019) Synthesis of CDs from β-Cyclodextrin for smart utilization in visual detection of cholesterol and cellular imaging. ChemistrySelect 4(48):14222–14227. https://doi.org/10.1002/slct.201903680
29. Zhu X, Wu M, Gu Y (2009) β-Cyclodextrin-cross-linked polymer as solid phase extraction material coupled with inductively coupled plasma mass spectrometry for the analysis of trace co (II). Talanta 78(2):565–569
30. Gnanarajan TP, Nasar AS, Iyer NP, Radhakrishnan G (2000) Synthesis of poly(urethane-imide) using aromatic secondary amine-blocked polyurethane prepolymer. J Polym Sci A Polym Chem 38(22):4032–4037. https://doi.org/10.1002/1099-0518(20001115)38:22<4032::Aid-pola30>3.0.Co;2-r
31. Chattopadhyay D, Mishra AK, Sreedhar B, Raju K (2006) Thermal and viscoelastic properties of polyurethane-imide/clay hybrid coatings. Polym Degrad Stab 91(8):1837–1849
32. Qu X, Alvarez PJ, Li Q (2013) Applications of nanotechnology in water and wastewater treatment. Water Res 47(12):3931–3946
33. Saberi A, Alipour E, Sadeghi M (2019) Superabsorbent magnetic Fe 3 O 4-based starch-poly (acrylic acid) nanocomposite hydrogel for efficient removal of dyes and heavy metal ions from water. J Polym Res 26(12):271
34. Yu L, Xue W, Cui L, Xing W, Cao X, Li H (2014) Use of hydroxypropyl-β-cyclodextrin/polyethylene glycol 400, modified Fe3O4 nanoparticles for Congo red removal. Int J Biol Macromol 64:233–239
35. Zhu Y, Hu J, Wang J (2012) Competitive adsorption of Pb (II), cu (II) and Zn (II) onto xanthate-modified magnetic chitosan. J Hazard Mater 221:155–161
36. Yuwei C, Jianlong W (2011) Preparation and characterization of magnetic chitosan nanoparticles and its application for cu (II) removal. Chem Eng J 168(1):286–292
37. Kiasat AR, Nazari S (2012) Magnetic nanoparticles grafted with β-cyclodextrin–polyurethane polymer as a novel nanomagnetic polymer brush catalyst for nucleophilic substitution reactions of benzyl halides in water. J Mol Catal A Chem 365:80–86
38. Fathi M, Entezami AA (2014) Stable aqueous dispersion of magnetic iron oxide core–shell nanoparticles prepared by biocompatible maleate polymers. Surf Interface Anal 46(3):145–151
39. Ranganath KV, Glorius F (2011) Superparamagnetic nanoparticles for asymmetric catalysis—a perfect match. Catal Sci Technol 1(1):13–22
40. Eibagi H, Faghihi K, Komijani M (2020) Synthesis of new environmentally friendly poly (urethane-imide) s as an adsorbent including β-cyclodextrin cavities and attached to iron nanoparticles for removal of gram-positive and gram-negative bacteria from water samples. Polym Test 90:106734
41. Faghihi K, Jalalian M (2008) Synthesis and characterization of new heat-resistance polymers based on N-(4-carboxy phenyl) trimellitimide and aromatic diamines. J Iran Chem Res 1(2):95–102
42. Can K, Ozmen M, Ersoz M (2009) Immobilization of albumin on aminosilane modified superparamagnetic magnetite nanoparticles and its characterization. Colloids Surf B: Biointerfaces 71(1):154–159
43. Ozaki S (1972) Recent advances in isocyanate chemistry. Chem Rev 72(5):457–496
44. Le HV, Ganem B (2011) Trifluoroacetic anhydride-catalyzed oxidation of isonitriles by DMSO: a rapid, convenient synthesis of isocyanates. Org Lett 13(10):2584–2585
45. Yoganathan S, Miller SJ (2013) N-Methylimidazole-catalyzed synthesis of carbamates from hydroxamic acids via the Lossen rearrangement. Org Lett 15(3):602–605
46. Solanki A, Sanghvi S, Devkar R, Thakore S (2016) β-Cyclodextrin based magnetic nanoconjugates for targeted drug delivery in cancer therapy. RSC Adv 6(101):98693–98707
47. Kiasat AR, Nazari S (2013) β-Cyclodextrin conjugated magnetic nanoparticles as a novel magnetic microvessel and phase transfer catalyst: synthesis and applications in nucleophilic substitution reaction of benzyl halides. J Incl Phenom Macrocycl Chem 76(3–4):363–368

48. Guo X, Wang J (2019) Comparison of linearization methods for modeling the Langmuir adsorption isotherm. J Mol Liq 296:111850
49. Deng J-H, Zhang X-R, Zeng G-M, Gong J-L, Niu Q-Y, Liang J (2013) Simultaneous removal of cd (II) and ionic dyes from aqueous solution using magnetic graphene oxide nanocomposite as an adsorbent. Chem Eng J 226:189–200
50. Li X, Wang S, Liu Y, Jiang L, Song B, Li M, Zeng G, Tan X, Cai X, Ding Y (2017) Adsorption of cu (II), Pb (II), and cd (II) ions from acidic aqueous solutions by diethylenetriaminepentaacetic acid-modified magnetic graphene oxide. J Chem Eng Data 62(1):407–416
51. Duan C, Zhao N, Yu X, Zhang X, Xu J (2013) Chemically modified kapok fiber for fast adsorption of Pb 2+, cd 2+, cu 2+ from aqueous solution. Cellulose 20(2):849–860
52. He J, Li Y, Wang C, Zhang K, Lin D, Kong L, Liu J (2017) Rapid adsorption of Pb, cu and cd from aqueous solutions by β-cyclodextrin polymers. Appl Surf Sci 426:29–39
53. Zhang Q, He M, Chen B, Hu B (2018) Magnetic mesoporous carbons derived from in situ MgO template formation for fast removal of heavy metal ions. ACS Omega 3(4):3752–3759
54. Kalaivani S, Muthukrishnaraj A, Sivanesan S, Ravikumar L (2016) Novel hyperbranched polyurethane resins for the removal of heavy metal ions from aqueous solution. Process Saf Environ Prot 104: 11–23
55. Fan L, Luo C, Sun M, Li X, Qiu H (2013) Highly selective adsorption of lead ions by water-dispersible magnetic chitosan/graphene oxide composites. Colloids Surf B: Biointerfaces 103:523–529
56. Zou Y, Wang X, Ai Y, Liu Y, Ji Y, Wang H, Hayat T, Alsaedi A, Hu W, Wang X (2016) β-Cyclodextrin modified graphitic carbon nitride for the removal of pollutants from aqueous solution: experimental and theoretical calculation study. J Mater Chem A 4(37): 14170–14179
57. Wang J, Guo X (2020) Adsorption kinetic models: physical meanings, applications, and solving methods. J Hazard Mater 390: 122156
58. Guo X, Wang J (2019) A general kinetic model for adsorption: theoretical analysis and modeling. J Mol Liq 288:111100